Transmission Electron Microscopy Analysis of $Cu(In,Ga)Se_2$ Solar Cell Materials

Chun Ming Li, Ian Robertson, and Angus Rockett
Department of Materials Science and Engineering, The University of Illinois
1304 W. Green St., Urbana, IL 61801

ABSTRACT

$Cu(In,Ga)Se_2$ (CIGS) and related materials in solar cell layers produced by the major U.S. manufacturers have been analyzed by transmission electron microscopy (TEM). Microstructural analysis shows a remarkably small number of dislocations in the materials with virtually none observable in some samples. Cu, In, Ga, S, and Se compositions observed by micro-energy dispersive spectroscopy (micro-EDS) lie along the pseudobinary Cu_2VI-III_2VI_3 tie line. Significant scatter is observable in the data. Remarkably, even for a 1 nm sampled area, the composition of grain boundaries matches the composition of the bulk grains to within the scatter in the data. Indeed, the centers of the scatter distributions are nearly identical. This indicates that grain boundaries do not exhibit altered stoichiometries.

1. General Introduction

Cu-Chalcopyrite $Cu(In,Ga)Se_2$ [CIGS] solar cells have the highest performances in both small area cells and large area modules of any thin film technology. However, several significant problems remain that hamper commercial application. Reproducibility has limited yields in manufacturing environments. Furthermore, materials produced by different techniques have strikingly different properties and solar cell performances in spite of appearing identical to many common analysis methods. Thus, the characteristics that distinguish a good solar cell material from an excellent one are not understood. The lack of a fundamental understanding of CIGS has hampered design of new processes and materials by which even higher performances can be obtained. Many of the issues that need to be resolved include the nanoscale structure and chemistry of the CIGS absorber layer and its surrounding grain boundaries, interfaces, and the heterojunction, which collects current. We report here preliminary results of a transmission electron microscopy (TEM) study of CIGS layers produced by two of the major U.S. manufacturers of CIGS thin film solar cells.

2. Experimental

Samples were obtained from Shell Solar Industries (SSI) and from Global Solar Energy (GSE). The Shell Solar samples were deposited on Mo-coated soda-lime glass from their standard process line and included significant composition gradients. The $Cu(In_{1-x}Ga_x)(S_ySe_{1-y})_2$ films included significant S both at the front and back of the layer and Ga primarily at the back of the device. The samples from GSE were deposited on Mo-coated stainless steel foils. These samples contained no S [y=0] but included Ga toward the back of the films.

Samples on glass substrates were prepared by the following sequence of steps. For plan view samples the glass substrate was thinned by mechanical grinding to a thickness of 20-30 μm. The samples were then ion milled to electron transparency. Care was required in the milling conditions to avoid redeposition of sputtered material onto the specimen. For cross-sectional samples, the preparation steps were 1) Sections were cut from the bulk material 2) sections were glued face-to-face 3) the glued sandwiches were cut into slices 4) specimens were thinned and smoothed by mechanical grinding, 5) samples were glued on a tripod polisher and the other side of the sample was ground to 20-30 mm thickness, 6) samples were glued to copper grids, 7) samples were ion milled to electron transparency.

Sample analysis was conducted in a Philips CM-12 TEM for general microstructural analysis or in a JEOL 2010F TEM for micro energy-dispersive X-ray analysis (micro-EDS). The JEOL instrument includes a field-emission source and can provide an electron beam probe size of less than 1 nm. The estimated probed volume in the micro-EDS analysis was ~1 nm. EDS analyses utilized the standard ZAF corrections for atomic number (Z), absorption (A) and fluorescence (F) of X-rays. A semi-quantitative result was obtained. Full quantitation of the results may be limited by the lack of a completely reliable composition standard. However, the compositions measured are what one would expect based on previous analyses of the samples in question by various techniques.

3. Results

A typical cross-sectional TEM image of a SSI device layer is shown in Fig 1. Individual grains are clearly visible with sizes of 400-800 nm. In spite of extensive searches, very few dislocations are observable within the grains of

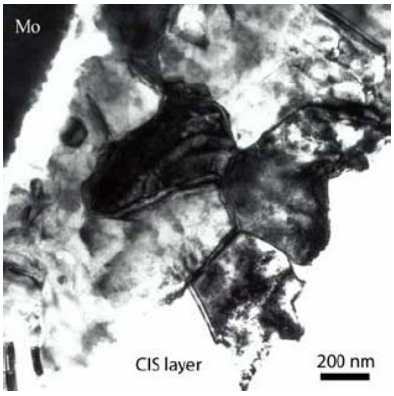

Figure 1. A typical TEM cross-sectional image of a SSI device layer. Grain boundaries are marked by Moir fringes and contrast changes. No dislocations are evident.

this material. Microtwins and stacking faults are not uncommon but are not present in all grains. The grain boundaries are evident from Moir fringes (which represent interference patterns between the atomic patterns in overlapping grains).

Compositions of individual grains and within grain boundaries were analyzed for both GSE and SSI samples. All analyses showed the presence of oxygen in moderate quantities. Compositions were, in general, consistent with compositions measured by secondary ion mass spectrometry, Auger electron spectroscopy, and bulk EDS analysis in a scanning electron microscope. The resulting compositions were analyzed to account for the presence of oxygen and results were plotted with and without the oxygen contribution to the composition on ternary phase diagrams. The results for the SSI and GSE samples are shown in Figure 2.

The ternary phase diagram results may be interpreted as follows. First, the grain and grain boundary points scatter about the same average compositions. Therefore there is no obvious difference in composition of the boundaries themselves. Grain boundaries could be expected to harbor a significant composition difference to compensate for dangling bonds in the boundaries. Indeed, it has been proposed that oxygen in grain boundaries is critical to improved device performance. The preliminary results clearly indicate this is not an important factor.

Both samples include a composition scatter lying roughly within a 10 atomic percent diameter of compositions. The GSE material is significantly more group III-rich than the SSI material (5% more group III and 5% less group I elements). However, the trends are essentially the same. The scatter is surprisingly large, especially when one considers the equilibrium phase diagram for the compounds. In particular, the SSI material includes significantly Cu-rich compositions. The very small probed volume (<1 nm diameter) combined with the large variation in composition observed and the lack of observable extended structural defects implies that the material can harbor large local composition variations without extended defects. This can explain the broad photoluminescence peaks. Future work will include measurements of point defect densities and organizations as a function of composition and will look for a correlation between such defects and device performances.

4. Conclusions

Preliminary results strongly suggest that grain boundary compositions in device polycrystals do not differ from bulk grain compositions even at the nanoscale. Extended defects are surprisingly rare even in materials produced by very different processes.

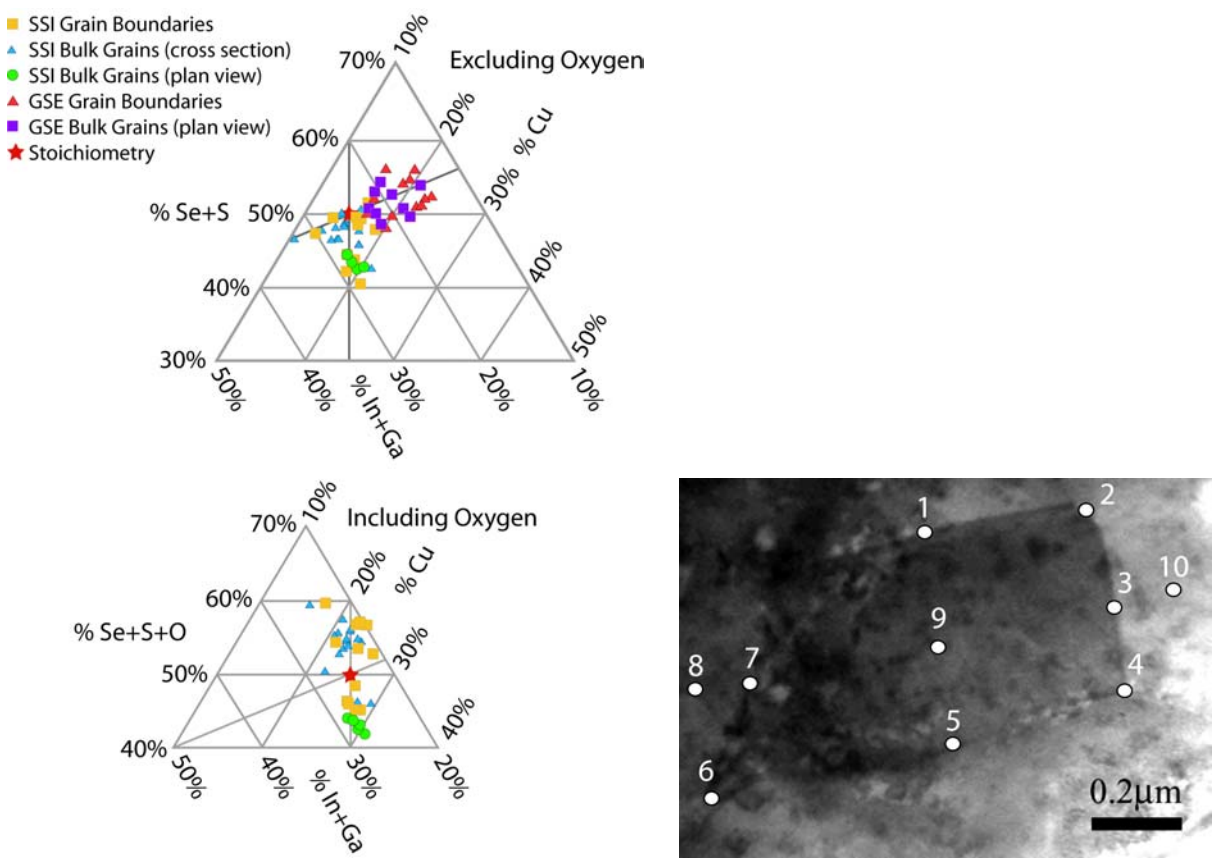

Figure 2: Shows the compositions measured in SSI and GSE absorber layers by micro-EDS. The upper ternary phase diagram shows the compositions measured excluding oxygen. The lower plot shows the same analyses for the SSI sample including oxygen. The comparison implies that oxygen is not participating in the chemical bonding of the compound. The inset image shows locations sampled in and around a SSI material grain in cross section.